Kinetics and reaction mechanism of isothermal oxidation of Iranian ilmenite concentrate powder

M. Mozammel, S. K. Sadrnezhaad, A. Khoshnevisan & H. Youzbashizadeh

Journal of Thermal Analysis and Calorimetry
An International Forum for Thermal Studies

ISSN 1388-6150

J Therm Anal Calorim
DOI 10.1007/s10973-012-2639-1

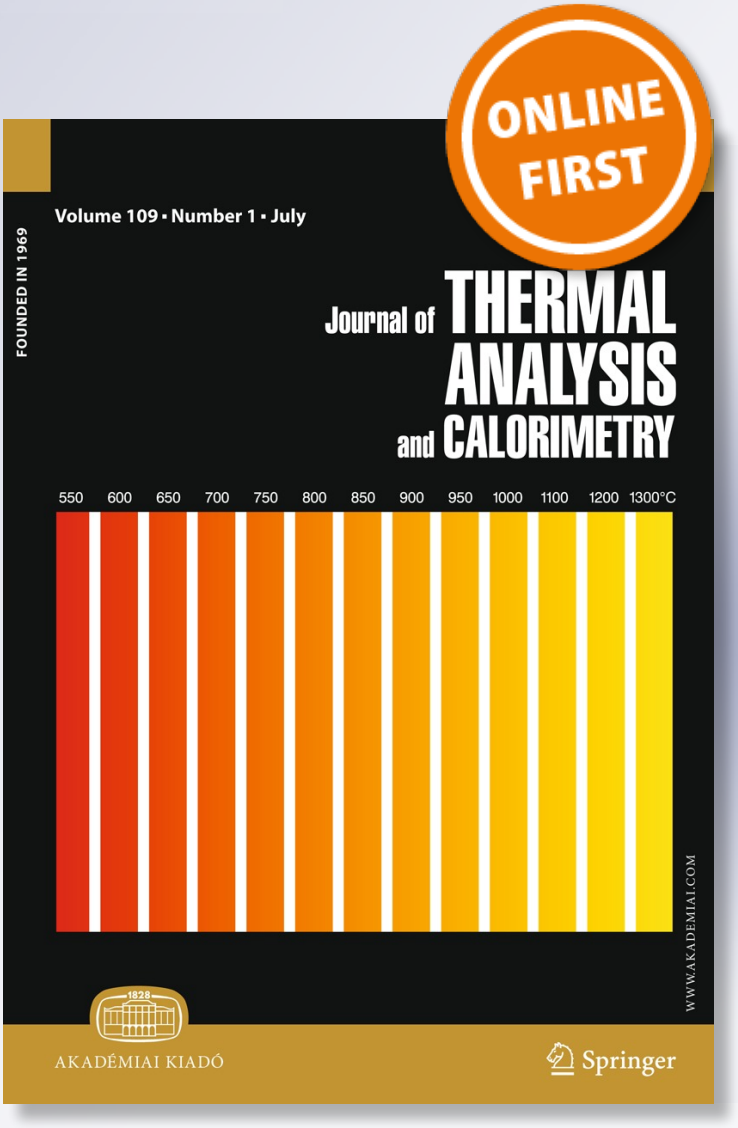

Springer

J Therm Anal Calorim
DOI 10.1007/s10973-012-2639-1

Kinetics and reaction mechanism of isothermal oxidation of Iranian ilmenite concentrate powder

M. Mozammel · S. K. Sadrnezhaad · A. Khoshnevisan · H. Youzbashizadeh

Received: 29 April 2012 / Accepted: 31 July 2012

Abstract Thermal oxidation of commercial ilmenite concentrate from Kahnouj titanium mines, Iran, at 500–950 °C was investigated for the first time. Fractional conversion was calculated from mass change of the samples during oxidation. Maximum FeO to Fe_2O_3 conversion of 98.63 % occurred at 900 °C after 120 min. Curve fit trials together with SEM line scan results indicated constant-size shrinking core model as the closest kinetic mechanism of the oxidation process. Below 750 °C, chemical reaction with activation energy of 80.65 kJ mol^{-1} and between 775 and 950 °C, ash diffusion with activation energy of 53.50 kJ mol^{-1} were the prevailing mechanisms. X-ray diffraction patterns approved presence of pseudobrookite, rutile, hematite, and $Fe_2O_3{\cdot}2TiO_2$ phases after oxidation of ilmenite concentrate at 950 °C.

Keywords Ilmenite · FeO · Isothermal oxidation · Kinetics · Thermal mass change · Phase transformation

Introduction

Ilmenite is an important source material of titania. It is usually extracted from magma rocks. With growth of titanium industry, gradual depletion of known reserves of natural rutile is taking place [1]. This has led to extensive efforts for conversion of still abundant ilmenite to what is known as synthetic rutile [2]. In recent years, there have been some efforts for using red mud with about 18 % TiO_2 to produce titanium dioxide [3, 4]. The conversion of ilmenite to synthetic rutile involves removal of iron species from ilmenite. There are two main processes for achieving this purpose: (1) production of a titanium-rich slag and reduction of its iron oxide to metallic iron and (2) removal of iron oxide by acid leaching [5–8]. These methods give synthetic rutile usable in TiO_2 chloride technology [9].

Different iron oxides of variable amounts are contained in natural ilmenite. Changeable rates of reduction are thus obtained. To fix these rates, natural ilmenite may first be oxidized and then be reduced to form metallic iron [10]. Many researchers have studied the oxidation process. Some have only looked at oxidation without discussing eventual reduction or leaching rates [11–14]. Others have discussed subsequent reduction and/or leaching rates plus morphology of the oxidized/reduced products as influenced by pre-oxidation [15–17]. Contradictions exist, however, between results of various researchers. Some have observed increasing maximum attainable reduction [16, 18], others have seen rate-increase of the iron oxide reduction [5, 19], a few have reported decreasing of the reduction temperature [5], and some others have recognized enhancement of the rate of leaching of the reduced iron [20–22]; all due to natural ilmenite pre-oxidation. Pistorius and Motlhamme [23] have observed enhancement of oxidation of ilmenite due to presence of water vapor during titanium-rich slag oxidation. Jones [18] and Janssen and Putnis [24] have concluded, on the other hand, that pre-oxidation has detrimental effects on subsequent reduction and leaching rates. Ogasawara and Veloso de Araujo [25] have reported that pre-oxidation has no significant effect on the leaching process.

Oxidation has also been used as a magnetizing roast for removal of chrome spinels from ilmenite concentrates [26]

M. Mozammel (✉) · S. K. Sadrnezhaad · A. Khoshnevisan · H. Youzbashizadeh
Department of Materials Science and Engineering, Sharif University of Technology, Azadi Avenue, P.O. Box 11155-9466, Tehran, Iran
e-mail: mozammel@mehr.sharif.edu

Published online: 06 September 2012

and to extract rutile from natural ilmenite ore [27]. The oxidation processes in the most of these researches were done by mechanochemical, fluidized bed, or TG method. Acid leaching of ilmenites of different origins has also been studied with both dilute and concentrated HCl [28, 29]. The affinity of ilmenite towards hydrochloric acid depends on its mineral nature and whether it has been altered or not. Altered and unaltered ilmenite mixtures containing in some cases rutile and leucoxene have been found in some deposits worldwide [30]. Inconsistencies in interpretation of physical structure and chemical composition of the utilized ilmenites, of course, exist among previous researchers [31].

Kinetics of reduction of ilmenite concentrates have been studied before [5, 18, 19, 32–34]. Jablonski and Prezepiera [35, 36] have focused on oxidation kinetics of Norwegian ilmenite concentrate and Canadian titanium slag using TG. They have concluded that contracting interfacial surface with activation energy of 30.88 kJ mol^{-1} has the main influence on the oxidation kinetics of the Norwegian ilmenite concentrate. Sun et al. [37, 38] have studied oxidation kinetics of pellet-shaped cement-bonded ilmenite in temperature range 800–1,000 °C. Based on un-reacted core data-analysis, they have found a mixed mechanism consisting of (a) intra-pellet oxygen diffusion, (b) intrinsic chemical reaction, and (c) heat transfer process. Poor heat conduction through the product shell had significant effect on the oxidation rate. They calculated rate constant and effective diffusivity in the temperature range 800–1,000 °C. They studied non-isothermal oxidation and reduction of synthetic ilmenite pellets in the temperature range 800–900 °C by dilute oxygen some years later. According to their results, shrinking core model described oxidation of synthetic ilmenite by intra-particle diffusion [39].

According to another study [13], oxidation of ilmenite powder during 10 h milling was describable by Eq. 1:

$$-\frac{\mathrm{d}(1-\alpha)}{\mathrm{d}t} = 2.1 \times 10^{-5} R^{2.44} a_c^{2.616} (1-\alpha)^2. \quad (1)$$

Rao and Rigaud [40] investigated the kinetics of the isothermal oxidation of both synthetic ilmenite powders and pellets for 6 h with pure oxygen and air. They found that the logarithmic rate was primarily obeyed. Activation energy for oxidation of ilmenite powder in the range of 507–704 °C was 8.5 kcal mol^{-1} (35.59 kJ mol^{-1}) with oxygen and in the range of 503–803 °C was 9.5 kcal mol^{-1} (39.71 kJ mol^{-1}) with air [40]. These authors have also investigated the oxidation of pellet-shape pressed ilmenite powder in the range of 600–970 °C. In this case, the rate of oxidation was parabolic and the activation energies were 20 kcal mol^{-1} (83.6 kJ mol^{-1}) in the temperature range of 612–802 °C and 43 kcal mol^{-1} (179.74 kJ mol^{-1}) in the temperature range of 848–970 °C.

In another study, the redox reactions during the oxidation and reduction of ilmenite powder have been investigated for chemical-looping combustion. In this study, ilmenite samples have been pre-oxidized for 24 h at 1,000 °C and then have several times been activated before beginning of the study. The oxidation of pre-oxidized ilmenite has been performed in the range of 800–950 °C by non-isothermal method. For oxidation reaction, the changing grain size model (CGSM) with chemical reaction control in the grains has been used to predict the solid conversion and to determine the kinetic parameters. The activation energies have been obtained ~11 kJ mol^{-1} for pre-oxidized and 25 kJ mol^{-1} for activated ilmenite [41].

From what mentioned above, it has become obvious that method of oxidation (continuous, isothermal, or mechanochemical oxidation) as well as the difference in physical structure (pellet or powder) and chemical composition of the utilized ilmenite play remarkable role in mechanisms of oxidation.

Most of these studies have been on compacted ilmenite pellets by non-isothermal continuous heating method. One of the two studies performed on pre-oxidized and activated ilmenite powder has been by non-isothermal heating [41] and the other on a *synthetic* ilmenite sample has been by isothermal method in the range of 503–803 °C [40]. The lack of published information about kinetics of isothermal oxidation of *natural* ilmenite concentrate *powders* above 803 °C becomes, therefore, obvious.

Information available in the literature on Iranian ilmenite is, on the other hand, extremely, limited [12, 42]. Importance of the origin of ilmenite on its kinetic behavior is clear from the above discussion. Since previous information is mostly related to the *synthetic* ilmenite powder oxidized for 6 h (in comparison with commercial powder oxidized in this study for 2 h), there exist enough impetus for our current study. This study was, therefore, focused on investigation of the oxidation kinetics of Iranian ilmenite concentrate via isothermal heating.

Experimental procedure

Materials

Commercial Kahnouj ilmenite concentrate produced via crushing, grinding and concentration processing of hard rocks were used as the starting raw material in this research. Chemical composition of the concentrate was as shown in Table 1. The mass ratio of titanium to iron in the concentrate was 0.74:1. Elemental compositions determined by XRF (Bruker S4 Explorer, Bruker AXS Karlsruhe, Germany) were used to evaluate compounds percentages. The Fe^{2+}/Fe^{3+} ratio was determined by

Table 1 Chemical composition of the ilmenite concentrate (mass%)

Composition	TiO_2	FeO	Fe_2O_3	MgO	SiO_2	CaO	Al_2O_3	MnO
Wt%	45.2	35.6	12.8	1.2	3.2	0.5	0.7	0.8

well-known analytical method [43]. As a result, the concentrate contained 75.16 % ilmenite and 4.84 % rutile.

Procedure

A sample of ilmenite concentrate was ground and dried before investigation. Particles of 63–80 μm diameter were separated by standard DIN sieves (DIN 4188) and dried at 250 °C in order to remove the moisture and volatile compounds to obtain a constant mass. The iron content of the concentrate had two Fe^{2+} and Fe^{3+} oxidation levels. Oxidation of the sample was investigated by thermal mass change method. Before measurement, samples of ilmenite were ground in a rotating disk mill. Investigations were carried out at temperatures ranging from 500 to 950 °C for at most 120 min. Mass of the samples was 100 mg. Alumina boats containing the samples were placed inside a muffle-type electric furnace for oxidation with 1 L min^{-1} blown air. Mass of the samples, dimension of the boats (2 cm × 7 cm), amount of powder (4.7 g cm^{-3}) and height of the concentrate in the boat (152 μm) resulted in less than 4 particle layers lying down on each other, taking the spaces between particles into account, assuring unlimited oxygen transfer through the concentrate bed. The air blow was chosen in order to eliminate the influence of outer diffusion factors on kinetics of process.

Samples of ilmenite concentrate were placed inside the furnace having a specified temperature for 20, 40, 60, 80, 100, and 120 min. Each sample was then taken out to cool down under argon atmosphere. It was weighed by Sartorius AG Gottingen scale (GC 1603 S-OCE, Germany). At each temperature the sample which was heated for 120 min, was selected for X-ray diffraction (XRD) to determine the structural changes. X-ray diffractometer (Bruker D8 Advance X-ray equipped with copper X-ray tube) was used for this purpose. Automatic divergence slit and 0.1 mm receiving slit were used for data collection. The X-ray tube operated at 40 kV and 35 mA. Intensity measurements were made at 2θ intervals of 0.02° in the angular range of $2\theta = 20°–80°$. Optical and scanning electron microscopy were performed to confirm the proposed oxidation mechanisms. SEM microscopy and EDS line scan were performed with VELA 3 XMH FIB-SEM (Tescan, USA). Plotting fractional conversion against time and temperature helped determining the mechanism of the oxidation reaction. From Arrhenius law, the activation energy of the reaction was evaluated.

Results and discussion

Phase transformation during oxidation

XRD experiments were performed to determine phase conversion during the oxidation reaction. XRD patterns of the raw and oxidized ilmenite (at 500, 700, and 950 °C for 2 h) are shown in Fig. 1. The first curve shows the XRD pattern of raw ilmenite concentrate at room temperature. It can be seen that the concentrate consists of ilmenite, hematite, and rutile. Combining XRF results with the mass balance data indicated the content of the concentrate to be 75.16 % ilmenite, 4.84 % rutile, and 11.6 % hematite, at the room temperature. After heating up to 500 °C, while the main phase was still ilmenite, a new phase had appeared according to the XRD spectrum. Based on the standard XRD cards, this was pseudorutile phase. It was, hence, concluded that at 500 °C, the ilmenite of the concentrate oxidizes to pseudorutile phase according to the following reaction:

$$3FeO{\cdot}TiO_2 + \frac{3}{4}O_2 \rightarrow Fe_2O_3{\cdot}3TiO_2 + \frac{1}{2}Fe_2O_3 m. \quad (2)$$

At 700 °C, ilmenite and pseudorutile XRD peaks shrank, while another new peak appeared. The new peak according to Gupta et al. [15] belongs to $Fe_2O_3{\cdot}2TiO_2$. This is a metastable intermediate phase which forms during heating of ilmenite and pseudorutile phase under oxygen at 700–1,000 °C [44]. It was, therefore, concluded that the ilmenite of the concentrate first converted into pseudorutile (Eq. 2) and then into $Fe_2O_3{\cdot}2TiO_2$ and rutile according to Eq. 3.

$$Fe_2O_3{\cdot}3TiO_2 \rightarrow Fe_2O_3{\cdot}2TiO_2 + TiO_2 \quad (3)$$

Since Eq. 2 was the sole accountable reaction which caused the mass gain of the concentrate, it was merely used for fractional conversion calculations and was used in kinetics mechanism determination. Pseudorutile phase was not detected by Janssen and Putnis [24] during heating of the ilmenite sample at 700 °C for 12 h. This may has been due to his prolonged heating metastable-phase conversion into hematite and rutile phases. This is consistent with the decrease in the intensity of the pseudorutile and ilmenite peaks occurring at longer times and higher temperatures of this study. At this temperature, other new peaks of hematite also appeared. This could be related to the decomposition of $Fe_2O_3{\cdot}2TiO_2$ to Fe_2O_3 and rutile according to Eq. 4 which would occur below 800 °C [15]:

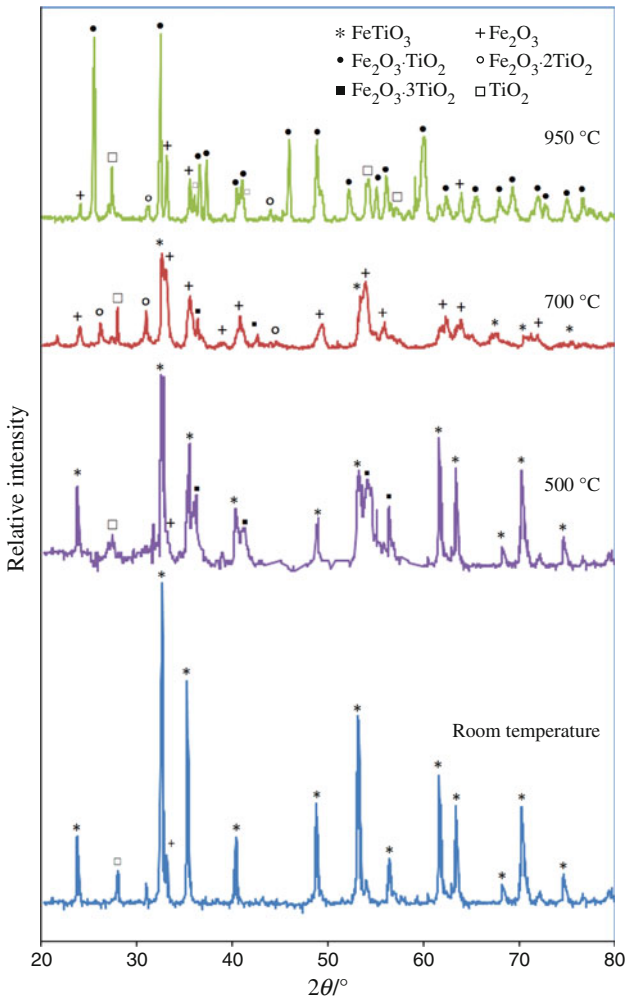

Fig. 1 XRD patterns of ilmenite concentrate oxidized at different temperatures for 2 h

$$Fe_2O_3{\cdot}2TiO_2 = Fe_2O_3 + 2TiO_2. \quad (4)$$

Increase in peak intensity of TiO_2 is also related to this reaction.

At 950 °C, the XRD pattern represented another new phase called pseudobrookite ($Fe_2O_3{\cdot}TiO_2$). Three possible reactions could have caused pseudobrookite formation:

a. Heating of Fe_2O_3–TiO_2 mixture in the presence of air [45, 46].
b. Decomposition of $Fe_2O_3{\cdot}2TiO_2$ to rutile and pseudobrookite above 800 °C [44].
c. Decomposition of $Fe_2O_3{\cdot}3TiO_2$ to rutile and pseudobrookite at 950 °C [16].

Navrotsky [45] has reported that temperature of 1,350 °C and duration of 72 h are required for process (a) to occur. Furthermore, the intensity of TiO_2 peak has not decreased at 950 °C. So TiO_2 has not been consumed by mechanism (a) to form pseudobrookite. Therefore, mechanism (a) could not be the pseudobrookite generating source, at 950 °C.

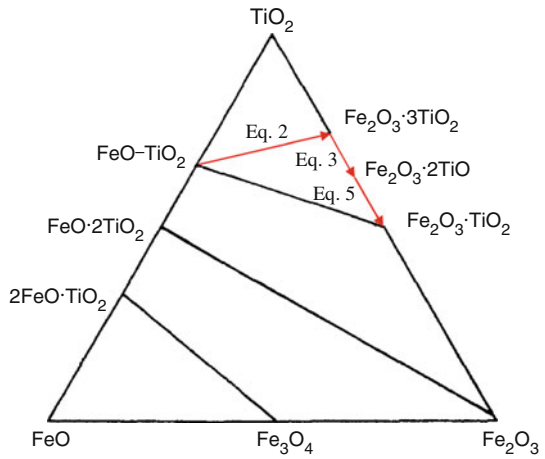

Fig. 2 FeO–Fe_2O_3–TiO_2 ternary diagram, as well as reaction pass at 950 °C

Disappearance of $Fe_2O_3{\cdot}3TiO_2$ decreases in intensity of $Fe_2O_3{\cdot}2TiO_2$ peaks and increases the intensity of TiO_2 peaks, all together. This indicates that mechanisms (b) and (c) are responsible for production of the pseudobrookite phase, at 950 °C.

It is concluded that at 950 °C, the ilmenite of the concentrate oxidizes to pseudorutile (Eq. 2) and then pseudorutile decomposes to $Fe_2O_3{\cdot}2TiO_2$ and rutile, according to the reaction 3. After this process, $Fe_2O_3{\cdot}2TiO_2$ decomposes to $Fe_2O_3{\cdot}TiO_2$ and rutile, according to Eq. 5. As it was specified, Eq. 2 is responsible for the mass gain and thus is used for kinetic evaluations.

$$Fe_2O_3{\cdot}2TiO_2 \rightarrow Fe_2O_3{\cdot}TiO_2 + TiO_2. \quad (5)$$

In the range 500–950 °C, reaction 2 is, hence, responsible for all the mass gain. $Fe_2O_3{\cdot}2TiO_2$ and $Fe_2O_3{\cdot}3TiO_2$ phases are metastable and their thermodynamic data corresponding to reactions 2–5 are not available.

At 950 °C, pseudobrookite accompanied with rutile, hematite, and $Fe_2O_3{\cdot}2TiO_2$ were present. These results were in agreement with Zhang et al. [16]. Gupta et al. [15] and Vasquez et al. [22] have not detected hematite at 1,000 °C, however. Figure 2 represents FeO–Fe_2O_3–TiO_2 [5] equilibrium diagram with reaction pass of ilmenite part of concentrate oxidation, schematically shown for 950 °C on the ternary system.

Effect of temperature on oxidation

As was shown in the previous section, the only reaction comprising mass gain is Eq. 2. The stoichiometric oxygen amount absorbed by the system (indicated as maximum mass gain in this article) is, thus, 3.956 % of initial

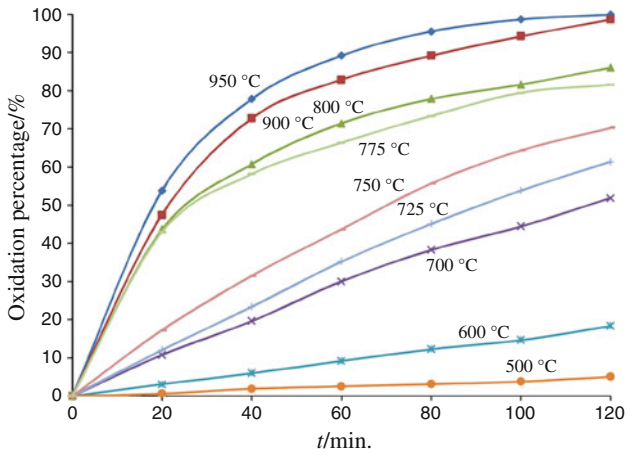

Fig. 3 Effect of temperature on the oxidation percentage of ilmenite concentrate

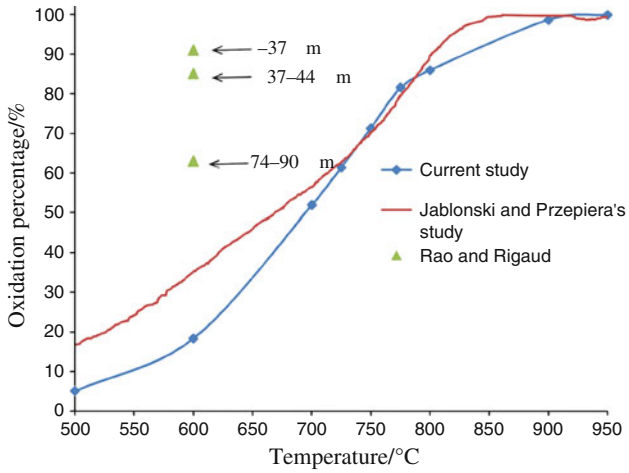

Fig. 4 Maximum oxidation percentage obtained at any studied temperatures after 120 min compared with Jablonsky and Przepiera [35] and Rao and Riggaud [40] data

concentrate mass according to Eq. 2. This calculated value is very close to the value obtained from the thermogravimetric experiment (3.949 % for oxidation of ilmenite concentrate at 950 °C for 2 h). The main mass gain observed during oxidation is, therefore, related to Eq. 2 and no other reaction may have considerable contribution. The mass increase of the ilmenite concentrate divided by the stoichiometric mass gain gives, hence, the oxidation fraction.

Effect of temperature on oxidation of ilmenite concentrate was investigated in the range of 500–950 °C. Results shown in Fig. 3 indicated that the oxidation amount increased with temperature. This increase was, especially, remarkable when temperature rise from 700 to 800 °C indicating a possible change of the rate controlling mechanism within this range. For this reason, temperature was increased by 25 °C intervals from 700 to 800 °C to focus on every possible compositional change within this specific range. The curves for these temperatures were added to Fig. 3.

Effect of temperature on the maximum attainable oxidation percentage is shown in Fig. 4. Maximum fraction for each temperature was assumed corresponding to 120 min oxidation (Fig. 3). The curve in this figure presents three distinct regions. From 500 to 600 °C, the oxidation percentage increases very slowly by the increase of oxidation temperature, but from 600 to 775 °C, the rate of oxidation percentage increase scales up very rapidly by the increase of temperature. Finally, after 800 till 950 °C, oxidation percentage rate slows down again. This trend has been observed by Vijay et al. [5] for ilmenite hydrogen reduction in fluidized bed reactor too. Shape of the curve resembles that given by Jablonski and Prezepiera [35]. The isothermal nature of this study which has been carried out at constant temperatures differs from that of the above researchers (carried out at 10 °C min^{-1}). The oxidation fractions obtained in this study are a bit less than those obtained by them, especially below 700 °C. Since the FeO contents of the concentrates used in both researches have almost been the same and the residence time for the present work was longer than that for the dynamic heating (i.e., 120 min against 95 min for dynamic heating), the only reason of the larger oxidation percentages of Jablonski and Prezepiera should be their smaller particle size (less than 40 μm in comparison 63–80 μm for present study). The smaller particle size has also caused the oxidation to be completed at 800 °C by their work, but the temperature of 950 °C was needed for the complete oxidation of ilmenite concentrate by present work. This explanation is in agreement with the Caplan et al. [47] report about the initial higher oxidation rate constant and lower activation energy for fine grained FeO scale which will reach a constant value as FeO coarsens with time.

When the results of Rao and Riggaud [40] were compared to recent study and the results of Jablonski and Prezepiera [35], very big differences were observed. As oxidation percentages data for powders were illustrated only in 610 °C by Rao and Rigaud, only one dot has been represented in Fig. 2 for particle sizes almost near to the particle sizes used by current (63–80 μm) and Jablonski and Przepiera's studies (−40 μm). These big differences are may be due to the synthetic nature of ilmenite samples used by Rao and Riggaud which were free from impurities which affected diffusion properties of oxygen into the ilmenite powder.

As the increase in the oxidation fraction from 900 to 950 °C was only 1.3 %. So 900 °C and 120 min of oxidation (98.63 % oxidation attained) were chosen as the best oxidation conditions of ilmenite concentrate from the economical point of view.

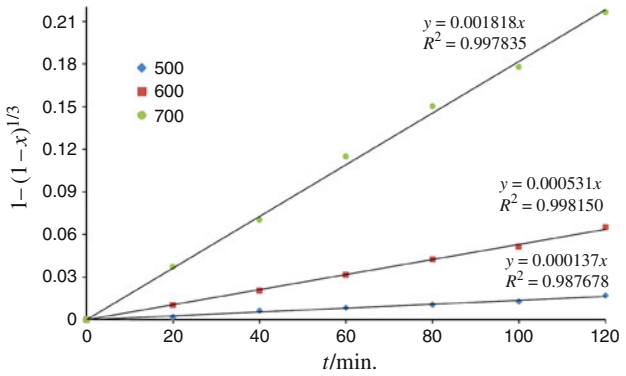

Fig. 5 Plots of $1-(1-X)^{1/3}$ (chemical reaction control plots) for the oxidation of ilmenite concentrate at temperatures 500–700 °C

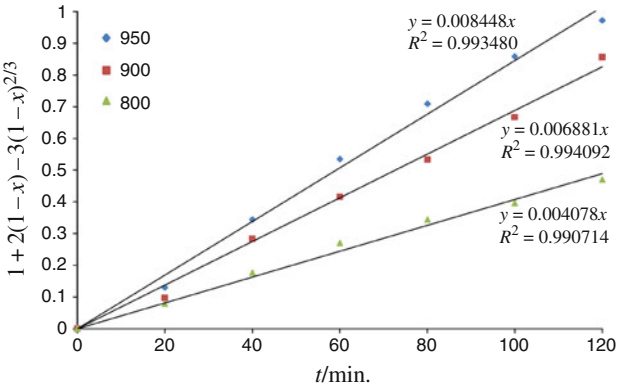

Fig. 6 Plots of $1+2(1-X)-3(1-X)^{2/3}$ (diffusion control plots) for the oxidation of ilmenite concentrate at temperatures 800–950 °C

Kinetics and reaction mechanism identification

The results obtained in Fig. 3 were examined by well-known kinetics models. Since the radius of the particles did not change during the oxidation process, so the shrinking core-constant particle size model was used to identify the reaction mechanism. There are some other articles in the literature which have selected the shrinking core model as the best describing model for the oxidation of ilmenite [38, 39]. According to the solid state kinetics models, if the reaction at the interface of particle core and newly formed product layer is the rate controlling step, the kinetics model would be:

$$1-(1-x)^{1/3}=k_c t. \tag{6}$$

And if the diffusion process is the rate controlling step, the kinetics model would be as follows [48]:

$$1+2(1-x)-3(1-x)^{2/3}=k_d t. \tag{7}$$

where x is the fraction oxidized at time t (min), k_c and k_d are apparent first order rate constants.

But if both chemical reaction and diffusion have a controlling influence on the reaction rate, the relation of the kinetics model would be of the following forms [33, 34, 49, 50]:

$$3k_1\left[1-(1-x)^{1/3}\right]+3/2k_2\left[1-2/3x-(1-x)^{2/3}\right]=t \tag{8}$$

$$\left[1-(1-x)^{1/3}\right]+y/6\left[(1-x)^{1/3}+1-2(1-x)^{2/3}\right]=k_M t \tag{9}$$

$$1-(1-x)^{1/3}+B\left[1-2/3x-(1-x)^{2/3}\right]=k_M t \tag{10}$$

where $B=k_c/k_d$, $k_M=2bMkC/\rho r^2$, $y=kd_0/2D_e$, D_e is the effective diffusivity, d_0 is the initial particle diameter, r is the radius of particles, b is the stochiometric coefficient, and k is the true rate constant.

Figures 5 and 6 show the mathematical fitting of the experimental data obtained during oxidation of ilmenite to the solid state kinetics equations in the range of 500–700 and 800–950 °C, respectively. Based on these results, it was found that below 700 °C chemical reaction was rate controlling step and above 800 °C diffusion through the product layer controlled the oxidation reaction. Mixed control mechanism was checked by relations 8–10, but a good fitting of the experimental data to these relations in the range of 500–950 °C (specially in the range of 700–800 °C) was not observed.

As was stated in the temperature effect section ("Phase transformation during oxidation" section), there was a remarkable increase in the oxidation amount, when the temperature increased from 600 to 700 °C. This could be related to the activation energy barrier which was overcome by the increase of temperature. Since the activation energy barrier has been overcome, the extent and the rate of ilmenite oxidation increased.

The other great increase in the oxidation amount which was observed as the temperature increased from 700 to 800 °C (Fig. 3), could be attributed to the change in the reaction rate controlling step from chemical reaction to diffusion through the product layer.

To investigate the rate controlling mechanism in the range of 700–800 °C, Eqs. 6 and 7 were applied to the related data in Fig. 3 to find the more accurate temperature range of mechanism change from chemical reaction to diffusion control. Figures 7 and 8 show mathematical fitting of oxidation data in the range of 700–800 °C to the chemical reaction and diffusion control models, respectively.

By studying the correlation coefficients of the linearization (Figs. 7, 8), it can be concluded that at 725 and 750 °C the chemical reaction control mechanism was dominated. But by increasing the temperature to 775 °C,

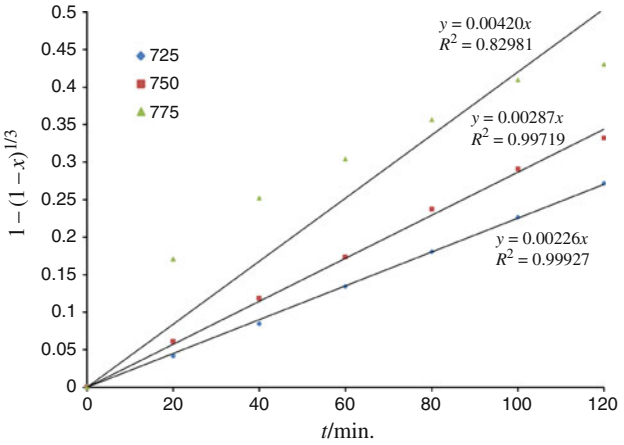

Fig. 7 Plots of $1 - (1 - X)^{1/3}$ (chemical reaction control plots) for the oxidation of ilmenite concentrate at temperatures 725–775 °C

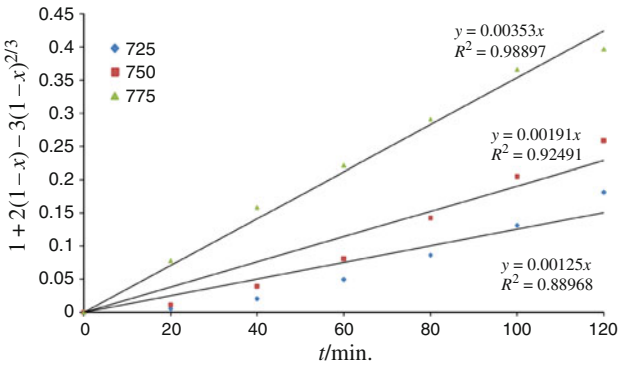

Fig. 8 Plots of $1 + 2(1 - X) - 3(1 - X)^{2/3}$ (diffusion control plots) for the oxidation of ilmenite concentrate at temperatures 725–775 °C

the dominated mechanism shifted to diffusion through the product layer.

The rate controlling mechanism is still unidentified at the temperature range of 750–775 °C.

Evaluation of activation energies

The relation between the overall rate constant and temperature may be expressed by the Arrhenius equation [48]:

$$k = A \exp(-E_a/RT) \quad (11)$$

where k is the overall rate constant ($m^2\ min^{-1}$), A is the frequency factor (min^{-1}), E_a is the activation energy ($J\ mol^{-1}$), R is the universal gas constant ($8.314\ J\ K^{-1}\ mol^{-1}$), and T is the reaction temperature (K).

In order to find the activation energy, the Arrhenius plot of $-\ln k$ as the function of T^{-1} was established at Fig. 9. The k values for different temperatures were extracted from slopes of lines in Figs. 5, 6, 7, and 8. From Arrhenius plots of Fig. 9, activation energies of 80.65 and 53.50 kJ mol^{-1},

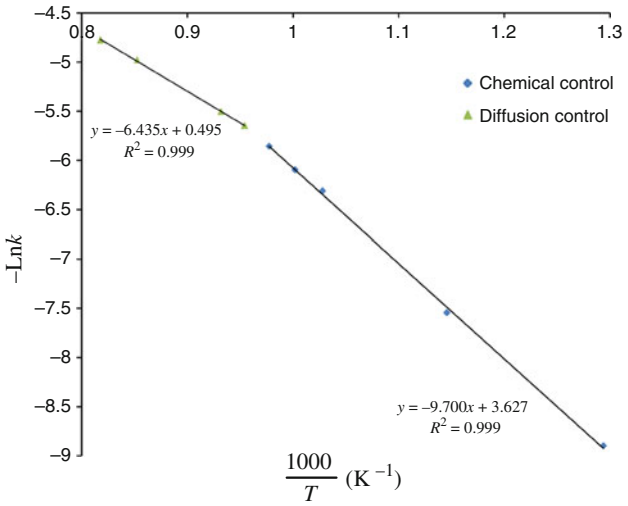

Fig. 9 Arrhenius plot of the data from Figs. 5, 6, 7, and 8

were calculated for the temperature ranges of 500–750 and 775–950 °C. The activation energy for both temperature ranges differs from the values reported in the literature by Jablonski and Przepiera [35] and Rao and Riggaud [40] which were 30.88 and 39.71 kJ mol^{-1}, respectively. It is for the first time that activation energy for the isothermal oxidation of ilmenite powders is published in the literature (specially for the range above 803 °C) as the value reported by Jablonski and Przepiera was obtained by continuous heating of ilmenite and that by Rao and Riggaud was obtained from a synthetic ilmenite in the range of 503–803 °C. These contradictions in the oxidation activation values confirmed the role of method of heating and concentrate nature, in the mechanism of reaction. This difference is even more remarkable when the evaluated activation energy is compared to what Abad et al. [41] reported (11 kJ mol^{-1}). This confirms that the pretreatment history (pre-oxidation and activation) of ilmenite powder before starting the tests has a very great influence on the activation energy and the kinetics of the ilmenite powder.

Both activation energies obtained by current study confirmed the rate controlling step declared for two different temperature ranges at previous section. Although it was stated somewhere else that the rate controlling mechanism of heterogeneous reactions is sometimes better predicted from kinetic models rather than activation energy values themselves [2].

Optical and scanning electron microscopy

As proposed kinetics mechanisms by both Rao–Riggaud and Jablonski and Przepiera differed from the mechanism declared by this study, scanning electron microscopy accompanied by optical microscopy was done to prove the

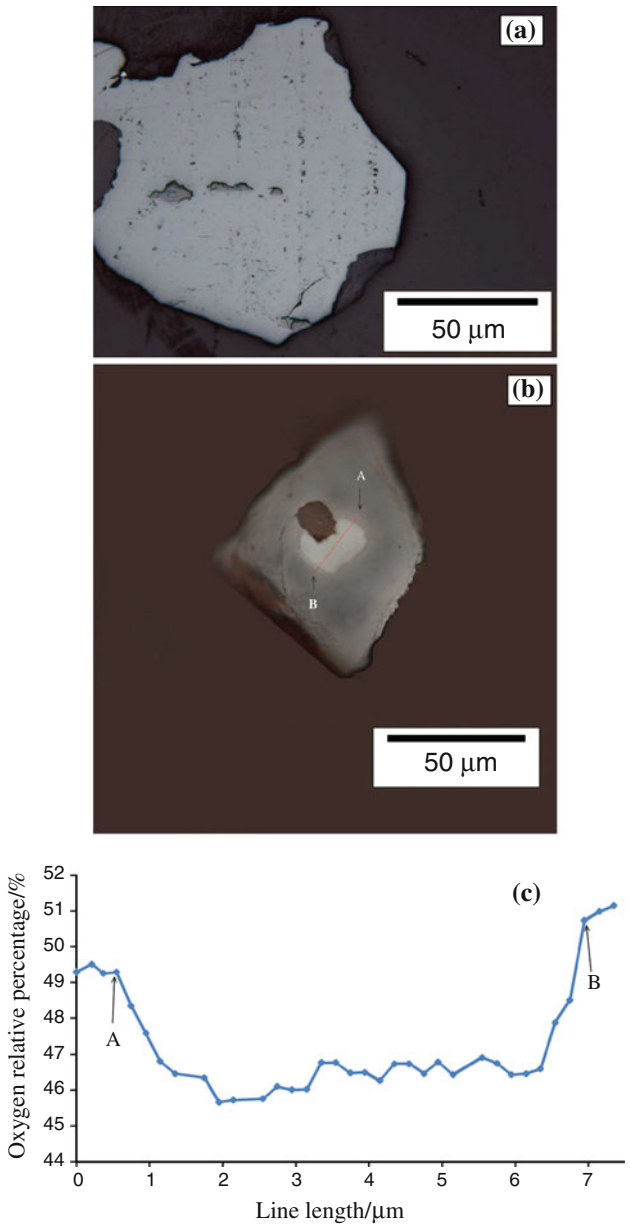

Fig. 10 **a** Not oxidized ilmenite particle, **b** A particle which was oxidized at 800 °C for 2 h, and **c** oxygen line scan curve according to **b** region (*A* to *B*)

proposed kinetics mechanism of ilmenite concentrate oxidation. Figure 10a shows a not oxidized particle of ilmenite concentrate. Figure 10b shows another particle which was oxidized at 800 °C for 2 h. It is evident that oxidation started from the outer surface of the particle and extended to its core. Therefore, the particle core remained not oxidized. To prove this fact a line scan was performed along the line as shown in Fig. 10b. It should be stated that due to the same atomic number of Fe and O for both FeO and Fe_2O_3 phases, the rim which was appeared in the optical microscopy image could not be detected by SEM. Accordingly, two images of optical and scanning electron microscopy were super imposed. This led to the possibility of illustrating the rim of oxidation reaction interface and the performed line scan simultaneously. The line scan result is shown in Fig. 10c. This figure shows that as the line enters to the not oxidized area, the oxygen percentage drops remarkably and by going out of it, increases again. This can be another reason which protects the proposed kinetics theory of shrinking core model to be the dominant mechanism during oxidation of ilmenite concentrate.

Conclusions

1. Oxidation at 900 °C for 120 min caused maximum mass gain with 98.63 % of FeO converting to Fe_2O_3.
2. Up to 750 °C, chemical reaction with activation energy of 80.65 kJ mol^{-1} and between 775 and 950 °C diffusion through the product layer with activation energy of 53.50 kJ mol^{-1} were rate controlling mechanism for ilmenite oxidation.
3. SEM–EDS line scan confirmed that the shrinking core model with constant particle size was the dominant mechanism for oxidation of ilmenite concentrate.
4. Raw material consisted of 75.16 % ilmenite, 4.84 % rutile, and 11.6 % hematite at room temperature. By increasing the oxidation temperature up to 500 °C, peaks pseudorutile compound appeared, although the main constituent phase still was ilmenite. At 700 °C, the intensity of ilmenite and pseudorutile peaks decreased while the new phase of $Fe_2O_3{\cdot}2TiO_2$ was appeared. At 950 °C, pseudobrookite accompanied by rutile, hematite, and $Fe_2O_3{\cdot}2TiO_2$ were the phases present.

References

1. Li WB, Yuan ZF, Xu C, Pan YF. Effect of temperature on carbothermic reduction of ilmenite. J Iron Steel Res Int. 2005; 12(4):1–5.
2. Olanipekun E. A kinetic study of the leaching of a Nigerian ilmenite ore by hydrochloric acid. Hydrometallurgy. 1999;53:1–10.
3. Pascual J, Corpas FA, Lopez-Beceiro J, Benitez-Guerrero M, Artiaga R. Thermal characterization of a Spanish red mud. J Therm Anal Calorim. 2009;96(2):407–12.
4. Atasoy A. An investigation on characterization and thermal analysis of the Aughinish red mud. J Therm Anal Calorim. 2005;81:357–61.
5. Vijay PL, Venugopalan R, Sathiyamoorthy D. Preoxidation and hydrogen reduction of ilmenite in a fluidized bed reactor. Metall Mater Trans B. 1996;27B(5):731–8.
6. Jablonski M, Przepiera A. Hazard in reaction of titanium raw materials with sulfuric acid. J Therm Anal Calorim. 2006; 83(3):571–3.
7. Jablonski M. Investigation of reaction products of sulfuric acid with ilmenite. J Therm Anal Calorim. 2008;93(3):717–20.

8. Jablonski M. Influence of particle size distribution on thermokinetics of ilmenite with sulphuric acid reaction. J Therm Anal Calorim. 2009;96:971–7.
9. Kucukkaragoz CS, Eric RH. Solid state reduction of a natural ilmenite. Miner Eng. 2006;19:334–7.
10. Sarker MK, Rashid AKMB, Kurny ASW. Kinetics of leaching of oxidized and reduced ilmenite in dilute hydrochloric acid solutions. Int J Miner Process. 2006;80:223–8.
11. Grey IE, Reid AF. Reaction sequences in the reduction of ilmenite: 3-reduction in a commercial rotary kiln; an X-ray diffraction study. Trans Inst Min Metall (Sect C). 1974;83:C39–46.
12. Akhgar BN, Pazouki M, Ranjbar M, Hosseinnia A, Keyanpour-Rad M. Preparation of nanosized synthetic rutile from ilmenite concentrate. Miner Eng. 2010;23:587–9.
13. Li C, Liang B. Study on the mechanochemical oxidation of ilmenite. J Alloy Compd. 2008;459:354–61.
14. Lanyon MR, Lwin T, Merritt RR. The dissolution of iron in the hydrochloric acid leach of an ilmenite concentrate. Hydrometallurgy. 1999;51:299–323.
15. Gupta SK, Rajakumar V, Grieveson P. Phase transformations during heating of ilmenite concentrates. Metall Mater Trans B. 1991;22B(5):711–6.
16. Zhang G, Ostrovski O. Effect of preoxidation and sintering on properties of ilmenite concentrates. Int J Miner Process. 2002; 64:201–18.
17. Xiong X, Yang Z, Ouyang H. Study on character of ilmenite modified by thermal treatment. Adv Mater Res. 2011;284–286:2090–3.
18. Jones DG. Kinetics of gaseous reduction of ilmenite. J Appl Chem Biotechnol. 1975;25(8):561–82.
19. Sun K, Takahashi R, Yagi JI. Reduction kinetics of cement-bonded natural ilmenite pellets with hydrogen. ISIJ Int. 1992; 32(4):496–504.
20. Roberts JMC. Ilmenite upgrading. Miner Mag. 1971;125(6):548.
21. Sarker MK, Kurny ASW. Effect of prior oxidation on the reduction and leaching of Bangladesh ilmenite. In: Proceedings of the international conference on recent advances of materials and minerals resources (RAMM 99), May 3–5. Malaysia: University of Sains; 1999. p. 712–722.
22. Vasquez R, Molina A. Leaching of ilmenite and pre-oxidized ilmenite in hydrochloric acid to obtain high grade titanium dioxide. In: 17th International metallurgical & materials conference proceedings: METAL 2008. Hradec nad Moravicí, Czech Republic, 13–15 May 2008, Europe.
23. Pistorius PC, Motlhamme T. Oxidation of high-titanium slags in the presence of water vapor. Miner Eng. 2006;19:232–6.
24. Janssen A, Putnis A. Processes of oxidation and HCl-leaching of Tellnes ilmenite. Hydrometallurgy. 2011;109:194–201.
25. Ogasawara T, Veloso de Araujo RV. Hydrochloric acid leaching of a pre-reduced Brazilian ilmenite concentrate in an autoclave. Hydrometallurgy. 2000;56:203–16.
26. Fisher-White MJ, Freeman DE, Grey IE, Lanyon MR, Pownceby MI, Sparrow GJ. Removal of chrome spinels from Murray Basin ilmenites by low temperature roasting. Miner Process Extr Metall Rev (Trans Inst Min Metall C). 2007;116(2):123–32.
27. Itoh S, Sato S, Ono J, Okada H, Nagasaka T. Feasibility study of the new rutile extraction process from natural ilmenite ore based on the oxidation reaction. Metall Mater Trans B. 2006;37BL:979–85.
28. Imahashi M, Takamatsu N. The dissolution of titanium minerals in hydrochloric and sulphuric acids. Bull Chem Soc Jpn. 1976;19(6):1549–53.
29. Tsuchida H, Narita E, Takeuchi H, Adachi M, Okabe T. Manufacture of high pure titanium (IV) oxide by the chloride process: 1. Kinetic study on leaching ilmenite ore in concentrated hydrochloric acid solution. Bull Chem Soc Jpn. 1982;55(6):1934–8.
30. Mackay TS. Acid leaching of ilmenite into synthetic rutile. Ind Eng Chem Prod Res Dev. 1974;13(1):9–18.
31. Francis AA, El-Midany AA. An assessment of the carbothermic reduction of ilmenite ore by statistical design. J Mater Process Technol. 2008;199:279–86.
32. Vries ML, Grey IE, Fitz Gerald JD. Crystallographic control in ilmenite reduction. Metall Mater Trans B. 2007;38B:267–77.
33. Wang Y, Yuan Zh. Reductive kinetics of the reaction between a natural ilmenite and carbon. Int J Miner Process. 2006;81: 133–40.
34. Wang Y, Yuan Z, Guo ZC, Tan QQ, Li ZY, Jiang WZ. Reduction mechanism of natural ilmenite with graphite. Trans Nonferrous Metal Soc. 2008;18:962–8.
35. Jablonski M, Przepiera A. Estimation of kinetic parameters of thermal oxidation of ilmenite. J Therm Anal Calorim. 2001;66: 617–22.
36. Przepiera A, Jablonski M. Thermal transformations of titanium slag of high titania content. J Therm Anal Calorim. 2003;74: 631–7.
37. Sun K, Takahashi R, Yagi JI. Nonisothermal behavior of the oxidation of natural ilmenite pellet. ISIJ Int. 1992;32(9):953–61.
38. Sun K, Ishii M, Takahashi R, Yagi JI. Oxidation kinetics of cement-bonded natural ilmenite pellets. ISIJ Int. 1992;32(4): 489–95.
39. Sun K, Takahashi R, Yagi JI. Kinetics of the oxidation and reduction of synthetic ilmenite. ISIJ Int. 1993;33(5):523–8.
40. Rao DB, Rigaud M. Kinetics of the oxidation of ilmenite. Oxid Met. 1975;9(1):99–116.
41. Abad A, Adanez J, Cuadrat A, Garcia-Labiano F, Gayan P, de Diego LF. Kinetics of redox reactions of ilmenite for chemical-looping combustion. Chem Eng Sci. 2011;66:689–702.
42. Pourabdoli M, Raygan SH, Abdizadeh H, Hanaei K. Production of high titania slag by electro-slag crucible melting (ESCM) process. Int J Miner Process. 2006;78:175–81.
43. Gennari FC, Andrade Gamboa JJ, Pasquevich DM. Formation of monoclinic Fe_2TiO_5 in the Fe_2O_3(s)–TiO_2(s)–Cl_2(g) system. J Mater Sci Lett. 1998;17:697–700.
44. Hunter RT, Edge M, Kaliveretenos A, Brewer KM, Brock NA, Hawkes AE, et al. Determination of the Fe^{2+}/Fe^{3+} ratio in nuclear waste glasses. J Am Ceram Soc. 1989;72:943–7.
45. Navrotsky A. Thermodynamics of formation of some compounds with the pseudobrookite structure and the Fe_2TiO_5–$FeTi_2O_5$ solid solution series. Am Mineral. 1975;60:249–56.
46. Gennari FC, Andrade Gamboa JJ, Pasquevich DM. Formation of pseudobrookite through gaseous chlorides and by solid-state reaction. J Mater Sci. 1998;33:1563–9.
47. Caplan D, Hussey RJ, Sproule GI, Graham MJ. The effect of FeO grain size and cavities on the oxidation of Fe. Corros Sci. 1981;21(9):689–711.
48. Levenspiel O. Chemical reaction engineering. New York: Wiley; 1972.
49. Ghosh MK, Das RP, Biswas AK. Oxidative ammonia leaching of sphalerite Part II: Cu(II)-catalyzed kinetics. Int J Miner Process. 2003;70:221–34.
50. Sahu SK, Sahu KK, Pandy BD. Leaching of zinc sulfide concentrate from the Ganesh–Himal deposit of Nepal. Metall Mater Trans B. 2006;37B:541–9.